IV Journeys in Multiphase Flows (JEM 2017)
March 27-31, 2017, São Paulo, SP, Brazil

Paper ID: JEM-2017-0014

PRESSURE DROP INDUCED BY AN ORIFICE PLATE ON A MIXTURE OF AIR AND WATER FLOWING HORIZONTALLY IN THE SLUG REGIME

Nathan da Costa Maidana
Faculty of Mechanical Engineering - University of Campinas, Rua Mendeleyev 200, 13083-860, Campinas, SP, Brazil
nathan@fem.unicamp.br

Eugênio Spanó Rosa
Faculty of Mechanical Engineering - University of Campinas, Rua Mendeleyev 200, 13083-860, Campinas, SP, Brazil
erosa@fem.unicamp.br

Abstract. An experimental analysis of the pressure drop induced by an orifice plate on a mixture of air and water flowing horizontally in slug regime is carried on. The pressure drop is not steady, but fluctuates around a mean value due to the intermittent nature of the slug flow. The analysis focus on the pressure drop mean value and its fluctuation around the mean value, the correlation between high and low pressure fluctuation and the occurrence of gas at the orifice throttle. Also the signal time and frequency domain are explored l. The experimental work is developed employing a fixed liquid and gas superficial velocities of 0.3 m/s and 0.5 m/s, respectively, and explore the effects of the area contraction ratio and the orifice plate distance from the air-water mixer.

Keywords*: orifice plate, pressure drop, air-water, slug flow*

1. INTRODUCTION

The two-phase flow behavior of a gas liquid mixture through valves, nozzles, orifices, pipe contractions or expansions and other pipe singularities is important for the control and operation of commonly found on power generation plants, refrigeration units, chemical reactors, depressurization emergency systems and on gas-oil production lines found on the petroleum industry.

The flow acceleration induced by a pipe singularity due to an area change continuously deforms the interfaces exhibiting an ever-changing void fraction near the singularity and back propagate pressure pulses upstream the orifice plate disturbing the two-phase flow structure as well. The design and control of pipe singularities require models to evaluate the pressure losses and the knowledge of the upstream and downstream effects on the gas-liquid flow properties, including the phase distribution and velocities.

Some of the reviewed works approached the gas-liquid flow of a mixture through orifices referencing only to the pressure drop regardless the flow pattern or the influence of the singularity on the two-phase flow structure. Chisholm (1983) develops pressure drop models based on the separated phase's models with and without slip, employing two-phase multipliers and compared against experimental data. Salcudean et al. (1983) analyzed pressure drop in various forms of flow obstruction geometries. Lin (1982) developed a model for flow measurement of gas-liquid flows using water and steam data and Kosajoy et al. (1997) developed a pressure drop model for a plate with multiple orifices and compared against R-113 experimental data. More recently, Fossa and Guglielmini (2002) developed a model to predict the pressure drop in orifices and compared against an air-water database with void fraction spanning from 20% up to 85%. The singularity were at 100D to 150D downstream the inlet. Oliveira et al. (2009) developed a comparative study among different models for mass measurements in gas-liquid flow based on orifice plates and compared against an air-water experimental data basis identifying the flow regime. The experimental data came from a test section with 0.021 m ID and the singularities were at 75D downstream the inlet.

There are quite a few works addressing to the flow structure in area contractions (Schmidt and Friedel, 1997; Fossa and Guglielmini, 1998; Bertola, 2004 and Chen et al., 2008) or in area expansions (Patrick and Swanson, 1959; Aloui et al., 1999; Ahmed, 2007), but the number of works addressed to the flow structure through orifices is reduced. Fossa et al. (2006) gives details of the flow structure of a horizontal air-water slug flow in the presence of an orifice plate. The test section is a 40 mm ID pipe with 300D long. The experimental setup used two orifices with area contraction ratio of 0.74 and of 0.54 with three distinct plate thickness. Using a multiple ring impedance sensor, the average void fraction was mapped upstream and downstream at distances up to 4D of the orifice edges. It was found that the void fraction peaks just downstream the orifice edge, furthermore the peak value increases as the orifice area contraction ratio decreases. Also was observed that the slug frequency slightly decreases for low contraction area ratios as the mixture velocity increases.

Zeghloul et al. (2015) explores the effect of an orifice on the upward air-water flow at the bubbly, slug and churn regimes. The vertical test section has 34mm ID and the orifice plate is installed 121D downstream of the inlet. The presence of the orifice plate changes significantly the flow structure at the neighborhood of the singularity but, the flow

recovers the upstream condition about 20D, 10D and 7D to bubbly, slug and churn regimes. The frequencies of the periodic structures are very similar upstream and downstream of the orifice for bubbly and slug regimes.

This work is primarily aimed at covering some gaps left by the foregoing investigations. One of them is the fact that the pressure drop is not steady, but it fluctuates around a mean value due to the intermittent nature of the slug flow. Another issue is the entrance length necessary to achieve a pressure drop measurement free from entrance effects. This is relevant since the pressure pulses propagating upstream may change the slug initiation process, which eventually modifies the pressure drop at the orifice.

The present analysis focus on the mean pressure drop and its fluctuation around the mean value, the correlation between high or low pressure fluctuation and the occurrence of gas at the orifice throttle and the characteristic frequencies of the pressure drop signal. The analysis is developed employing a fixed liquid and gas superficial velocities of 0.3 and 0.5 m/s, respectively and explores the effects of an area contraction ratio and the orifice plate distance from the air-water mixer.

2. EXPERIMENTAL PROCEDURE AND DATA PROCESSING

The horizontal experimental test section has a 26 mm ID straight pipe made of transparent acrylic with 26.24 m long or 1009 D, see Figure 1. The working fluids are compressed air and water at ambient conditions, nearly 93.7 kPa and 25 ^{o}C. The water density and viscosity are 998 kg/m^3 and 0.001 Pa.s while the air was treated as an ideal gas with R equals to 286.9 J/kgK. Three compressors and a centrifugal pump supply the air and the water to the mixer installed at the entrance of the test section. The air and the water flow rates are measured separately employing a homemade sonic nozzle and a Metroval Coriolis mass type flow meter respectively. The air-water mixer consists of a pipe section divided in two by an internal split plate. The water is injected at the bottom section while the air at the top section. The air and the water streams flow in parallel at a distance equivalent to ten pipe diameters before mixing. At the end of the test section, the air-water mixture is discharged into a receiving tank with 3 m^3 in volume open to the atmosphere. The air vents to the atmosphere and the liquid, free of air bubbles, is pumped back to the test section.

The test section has four measuring stations identified by S1, S2, S3 and S4 respectively located at 153 D, 307 D, 551 D and 870 D downstream the air-water mixer. Each measuring station has a pressure transducer and a twin set of house-made single wire conductive probes axially spaced of 112.5 mm. The conductive probes have an output voltage, V_m, which spans between low and high values, V_{low} and V_{high}. These extremes, V_{low} and V_{high}, correspond when the test section is full of gas or full of liquid, respectively. The conductive probes have an output dimensionless voltage, 1-V*, proportional to the cross section's void fraction of the air-water flow (Rosa and Souza, 2015) defined as:

$$V^* = \frac{V_m - V_{low}}{V_{high} - V_{low}} \quad \textbf{(1)}$$

Each orifice plate is tested at three axial positions along the test section. These positions are identified by Setup A, B and C and represent the axial positions of 169 D, 632 D and 886 D downstream the mixer. Table 1 briefs the distances relative to the mixer or relative to the orifice plate position in setups A, B and C. For example: the 2nd line informs that the orifice plate in setup C is at 886 D downstream the mixer; the 4th line says that the measuring station #2 is at 325 D upstream the orifice plate in setup B.

Table 1. Distances in multiples of the pipe diameter. Second line displays the distances from the measuring stations and the orifice plates for setups A, B and C in regard to the mixer. The next three lines have as reference the position of the orifices at A, B, and C.

Distances	mixer	#1	A	#2	#3	B	#4	C	outlet
from the mixer	0	153D	169D	307D	551D	632D	870D	886D	1009D
from orifice at A	-169D	-16D	0	138D	382D	-	701D	-	840D
from orifice at B	-632D	-479D	-	-325D	-81D	0	238D	-	377D
from orifice at C	-886D	-733D	-	-579D	-335D	-	-16D	0	123D

Three stainless steel orifice plates with throat diameter, d, are used with area contraction ratios, $\sigma = (d/D)^2$, of 0.250, 0.123 and 0.072. Each orifice has a concentric circular hole, with squared edges with thickness, t, of 3mm. The thickness to orifice diameter ratio, t/d, is of 0.231, 0.330 and 0.429, which results in thin orifice plates accordingly to Chisholm (1983). A differential pressure transducer measures the pressure drop across the orifice plate through flange taps which are 0.008 m at the upstream and downstream faces of the plate.

The analogical signals of the twin conductance probes and of the pressure at each measuring station and at the orifice plate are sampled at 3 kHz and digitized employing, respectively, two NI 9203 analog input modes and a NI cDAQ-9188 chassis, both from National Instruments.

During the preliminary tests of the experimental apparatus, it was observed large pressure pulses back propagated from the orifice plate, which caused fluctuations on the air and water inlet flow rates. To avoid the undesired inlet fluctuations two procedures were adopted: the use of a sonic nozzle to measure the air flow rate and operate the centrifugal pump at the maximum speed and the use of an inlet choke to set the desired water flow rate. A quite stable inlet air flow rate was obtained operating with the sonic nozzle. The large pressure drop at the inlet choke of the water line minimized the inlet water fluctuations to less than 4% of the nominal flow rate.

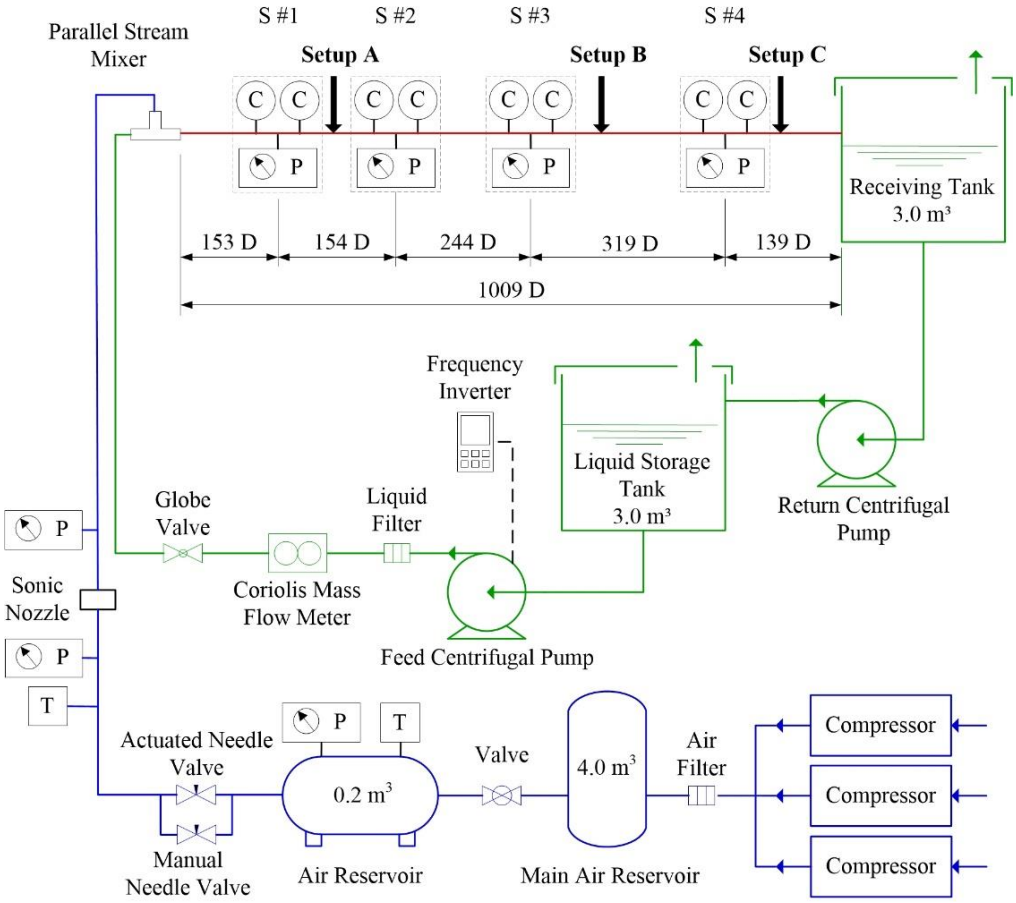

Figure 1. Experimental Apparatus. Letters A, B and C at the red line represent the axial location of the orifice plate, measuring 169 D, 632 D and 882 D downstream the stream mixer, respectively. (adapted from Dalla Maria, 2016)

The inlet water and air flow rates are expressed in terms of their superficial velocities, J_L and J_G defined as the ratio of the volumetric phase flow rate by the pipe cross section area. The nominal water and air superficial velocities, J_L and J_G, are 0.30m/s and 0.50m/s, respectively. The chosen values assure a representative quantity of unit cells. An increase on the gas flow rate would lead to larger bubbles and the test section would have few bubbles to be representative for the bubble-to-bubble interaction of slug flow.

The test grid, shown in Table 2, consists of four series. The first employs a straight pipe without orifice plate used as a reference state and the other three series correspond to each orifice plate with area contraction ratio, σ, of 0.250, 0.123 and 0.072. Each series consists of 10 runs for each setup. The experimental work amounts to 100 runs. Each individual run has the liquid and gas inlet flow rates carefully adjusted to nominal values. Before starting the data acquisition, is necessary to give a time delay of nearly 30s until the effects of the changes on the inlet flow rates exits the test section. Each run lasts for 120s. The sampling data consists of 13 channels corresponding to the conductance probes and the pressure for measuring stations #1 to #4 plus the orifice plate pressure difference.

The correlation between high or low pressure fluctuation at the orifice and the occurrence of liquid or gas phase at the orifice throttle is established employing a simultaneous measurement of the pressure drop and the void fraction using a contact needle probe. The contact needle probe is composed by a non-insulated gold wire with a diameter of 108 µm. The gold wire is housed by a stainless steel needle with external diameter of 900 µm, which gives structural

support to the gold wire and proves ground to the electronic circuit. The measurement of the contact needle probe is used to evaluate local void fractions and a micrometer is responsible to set the radial position of the probe. More details about the conductive probes located at the measurement stations, the contact needle probe and the electronic circuit is available in Rosa and Souza (2015).

Table 2. Test grid displaying for each area contraction ratio, measuring station and setup. The sampled number of slug units, the liquid and gas superficial velocities are shown.

	Mes. Station	Setup A			Setup B			Setup C		
		Units	J_L	J_G	Units	J_L	J_G	Units	J_L	J_G
		-	m/s	m/s	-	m/s	m/s	-	m/s	m/s
Straight Pipe	#1	939	0.30	0.49	939	0.30	0.49	939	0.30	0.49
	#2	789	0.30	0.50	789	0.30	0.50	789	0.30	0.50
	#3	649	0.30	0.50	649	0.30	0.50	649	0.30	0.50
	#4	618	0.30	0.51	618	0.30	0.51	618	0.30	0.51
$\sigma = 0.250$	#1	721	0.30	0.50	595	0.30	0.49	627	0.30	0.49
	#2	692	0.30	0.51	591	0.30	0.49	582	0.30	0.50
	#3	653	0.30	0.52	508	0.30	0.50	502	0.30	0.50
	#4	635	0.30	0.53	445	0.30	0.51	492	0.30	0.50
$\sigma = 0.123$	#1	478	0.30	0.50	474	0.30	0.48	564	0.30	0.49
	#2	509	0.30	0.54	428	0.30	0.48	476	0.30	0.49
	#3	460	0.30	0.54	359	0.30	0.49	392	0.30	0.50
	#4	480	0.30	0.56	389	0.30	0.53	312	0.30	0.50
$\sigma = 0.079$	#1	322	0.30	0.50	456	0.30	0.49	585	0.30	0.50
	#2	380	0.30	0.62	401	0.30	0.49	495	0.30	0.50
	#3	390	0.30	0.63	309	0.30	0.51	362	0.30	0.51
	#4	374	0.30	0.63	355	0.30	0.62	258	0.30	0.51

3. EXPERIMENTAL RESULTS

The time record of the pressure difference across the orifice plates is displayed on Figure 2 for setups A, B, and C and for area contraction ratios, σ, of 0.250, 0.123 and 0.072 for (J_L, J_G) of (0.30; 0.50) m/s. The outmost feature of these signals is the pulsatile behavior. The pressure difference exhibits a constant mean value, but the signal fluctuates around the mean. This fluctuating feature is associated to the passage across the orifice of mixtures rich in liquid phase alternated by mixtures rich in gas phase typical of slug flow.

The influence of the area contraction ratio is observed comparing the signals displayed on Figure 2 from left to right. As σ decreases, the mean value increases and so does the amplitude of the fluctuations. This is expected since the area of the orifice is decreasing. The influence of the distance from the orifice plate to the gas liquid mixer is perceived comparing the signals at constant σ. The samples taken the same time interval indicates that the number of peaks and valleys decreases as the distance from the mixer increases from 169D to 632D and from 632D to 886D corresponding, respectively, to setups A, B and C.

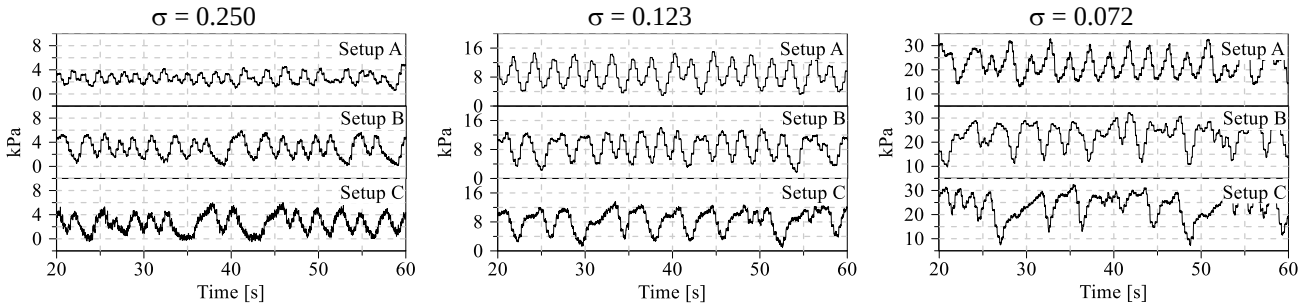

Figure 2. Pressure difference across the orifice plate versus time for setups A, B and C for area contraction ratios of 0.250, 0.123 and 0.07 from left to right respectively. Phases flow rates: (J_L, J_G) of (0.30; 0.50) m/s.

Figure 3 displays the simultaneous time records of the pressure difference across the orifice plate and the signal of the contact needle probe, placed at the piper center line but at 0.008 m downstream the plate's face. The data applies to setup B for σ of 0.123 and 0.072 for (J_L, J_G) of (0.30; 0.50) m/s. To aid the analysis a dashed line is added on the figures representing the mean pressure difference. The output of the contact needle probe is a dimensionless voltage,

V*, which spans from 1 to 0. V* equals to 1 means 100 % water and 0 means 100% gas. Using this information is possible to correlate the pressure fluctuation above or below the mean value to the passage of liquid or gas phases through the orifice plate. Figure 3, disclose that the instantaneous pressure differences above the mean pressure difference are associated to a gas-liquid mixture rich on the liquid phase or one with low void fraction. Conversely, instantaneous pressure differences below the mean pressure difference are associated to a mixture rich on the gas phase or one with high void fraction.

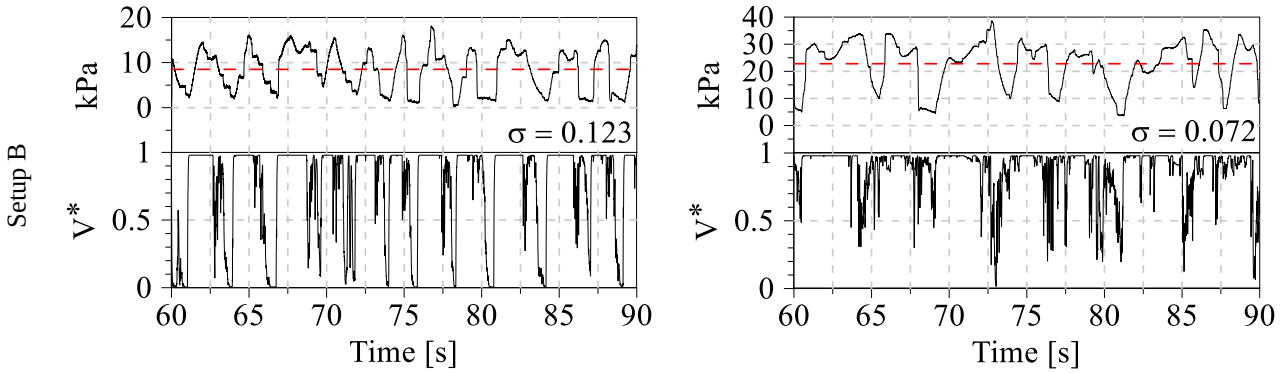

Figure 3. Comparison of the time records of the pressure difference across the orifice against the output of the contact needle probe placed at 0.008 m downstream the orifice centerline employing setup B and area contraction ratios of 0.123 and 0.072. Phases flow rates: (J_L, J_G) of (0.30; 0.50) m/s.

The pressure fluctuation around the mean pressure difference across the orifice is shown in Figure 4 as PDFs of ΔP_f defined as the difference between the instantaneous pressure difference and its mean value. Therefore, if $\Delta P_f < 0$ means that the instantaneous pressure difference is lower than the mean pressure difference. The figure compares the fluctuation PDF at distinct distances from the gas-liquid mixer for each σ of 0.250, 0.123 and 0.072. For the orifice with σ = 0.250 the fluctuations are symmetrical and show a slightly tendency to increase the spread as the distance from the mixer increase. As the area contraction ratio decreases to σ = 0.123, the PDFs are no longer symmetrical but exhibits a shape more similar to a top hat distribution. Despite the difference in shape among these PDFs and the ones with σ = 0.250, the spread is only slightly greater than the former PDFs. An additional decrease on σ to 0.072 leads to positive skew PDFs and an increase on the spread of the PDFs.

The PDFs of ΔP_f have mean values coincident with zero because the mean value of the instantaneous fluctuations is by definition null. Using this property is possible to state that the probability of occurrence of pressure fluctuations on the interval from $-\infty < \Delta P_f < 0$ and from $0 < \Delta P_f < +\infty$ are of 50% each. Since $\Delta P_f < 0$ represent a mixture rich in gas while $\Delta P_f > 0$ is a mixture rich in liquid, them is possible to conclude that at the neighborhood of the orifice the likelihood of a mixture rich in gas or liquid phases are always equal no matter the distance from the gas-liquid mixer neither the area contraction ratio. In other words, near the orifice there is a redistribution of the gas and liquid in such way that the chances of occurrence of low and high void fractions are always balanced.

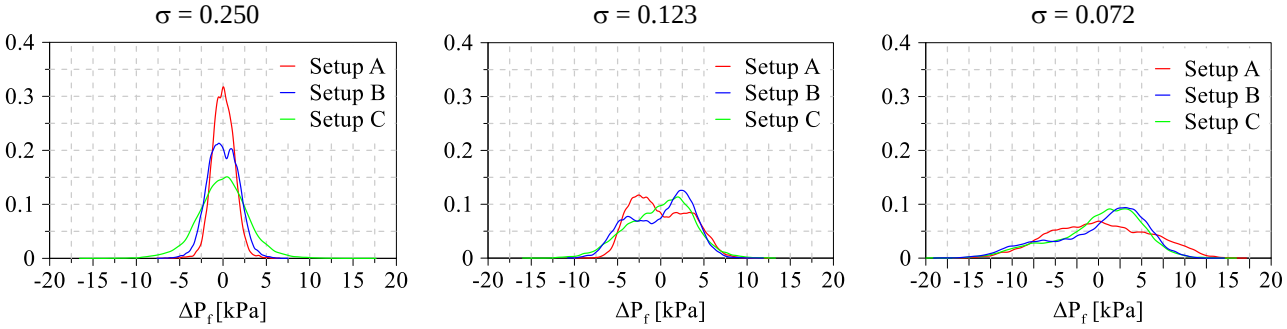

Figure 4. PDFs of the pressure fluctuation across the orifice plate on setups A, B and C for area contraction ratios of 0.250, 0.123 and 0.072, from left to right, respectively. Phases flow rates: (J_L, J_G) of (0.30; 0.50) m/s.

The power spectral densities of the pressure difference across the orifice plates with σ of 0.250, 0.123 and 0.072 for setups A, B and C are displayed on Figure 5. For orifice with σ of 0.250 on setups A, B and C it is observed a frequency band spanning from 0.1 Hz to 0.7 Hz with tendency to displace to low frequencies as the distance from the mixer increases. Considering that the setup A is at 169D downstream the mixer, the former being closer to the gas-liquid mixer has less chances to have interaction between neighboring bubbles and change velocities and lengths therefore it has more defined frequencies and the highest frequencies. On the other hand, setup C has the orifice plate at 886D

downstream the mixer. At these distance, the slug flow has the chance to interact before going through the orifice plate. But not only this, it is also expected a line with several bubbles separated by liquid pistons behaving like a large oscillator with dissipation due to the wall shear stress. It is supposed that this large distance favors the appearance of low frequency range and cuts off the high frequencies due to the neighboring bubbles interaction. Lastly, the orifice with σ of 0.250 has the lowest energy levels indicating that the pressure disturbances induced by the orifice plate are weak when compared with the energy level as σ diminishes.

Comparing the PSD of the pressure difference at the orifice plates with σ = 0.123 and 0.072 it is possible to disclose that the frequency band changes with the distance from the mixer and is not characterized by a single frequency. The signals with highest energy belong to the orifice plates closer to the gas-liquid mixer (setup A). The PSD energy decreases as the distance from the mixer increases, as seen for setup B and C.

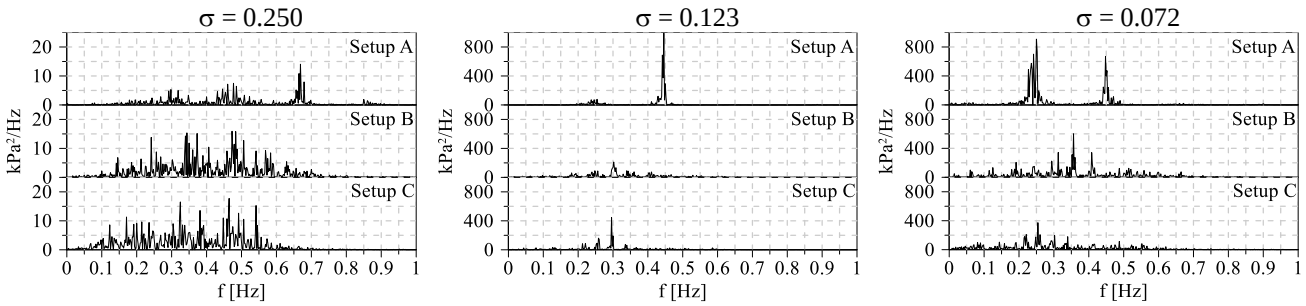

Figure 5. Power spectral density of the pressure difference across the orifice plates for setups A, B and C with area contraction ratios of 0.250, 0.123 and 0.072. Phases flow rates: (J_L, J_G) of (0.30; 0.50) m/s.

For referencing purposes, Table 3 displays the numerical values of the mean pressure difference across the orifice and its fluctuation is defined as twice the standard deviation. The table displays data as function of the area contraction ratio and of the setups types. The central area of the table displays the mean value and the fluctuation separated by a slash. The bottom row displays the average values. The aim of Table 3 data is to support the qualitative aspects highlighted on the previous paragraphs.

Table 3. Pressure difference at the orifice and the RMS of the pressure difference fluctuations are presented at the 2nd through 4th lines in kPa for σ of 0.250, 0.123 and 0.072 and Setups A, B and C. Phases flow rates: (J_L, J_G) of (0.30; 0.50) m/s.

	σ = 0.250	σ = 0.123	σ = 0.072
Setup A	2.6/±1.8	8.6/±6.4	22.0/±10.2
Setup B	3.0/±2.6	8.4/±6.8	22.8/±10.4
Setup C	2.6/±2.6	8.3/±5.6	23.5/±9.2
Average	2.7/±2.4	8.5/±6.2	22.8/±9.8

A visual inspection on Table 3 discloses that the mean pressure difference across the orifice plate depends on the area contraction ratio but not on the distance from the mixer. This evidence suggests that the gas-liquid flow rearranges at the vicinity of the orifice in such way that the pressure difference remains the same regardless the distance from the mixer. This feature is supported by the equal odds for mixtures rich in gas and liquid phases.

The mean pressure drop, ΔP_M , increases as σ decreases. Figure 6 shows the growth rate of the dimensionless pressure drop, ΔP_M^*, as a function of the reciprocal area contraction ratio. The dimensionless pressure drop is expressed in the form:

$$\Delta P_M^* = \frac{\Delta P_M}{\frac{1}{2}\rho_h J^2} \tag{2}$$

where ρ_h refers to the mixture density based on the homogenous flow. For the experimental data, $\alpha_h = 0.625$ and $\rho_h = 375$ kg/m^3. Lastly J is the mixture superficial velocity, $J = J_L + J_G = 0.8$ m/s. Figure 6 exhibits a linear growth rate of ΔP_M^* against $(1/\sigma)^2$.

The pressure fluctuation around the mean pressure drop increases as σ decreases. For convenience, Figure 6 shows the pressure fluctuation to the mean pressure drop ratio as a function of the reciprocal σ. The figure discloses a decreasing rate of the pressure ratio against $(1/\sigma)^2$.

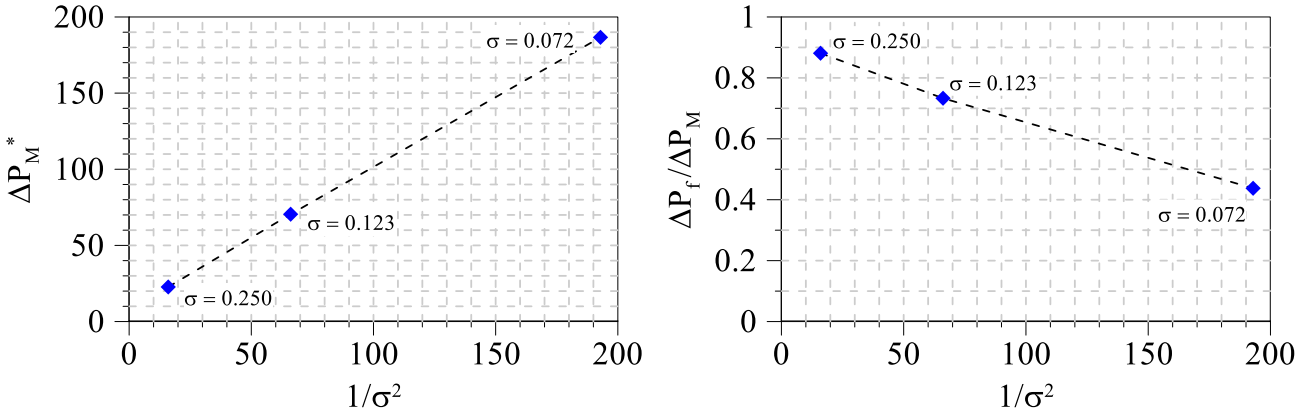

Figure 6. Dimensionless pressure drop across the orifice and pressure fluctuation to mean pressure drop ratio against the orifice area contraction ratio. Phases flow rates: (J_L, J_G) of (0.30; 0.50) m/s.

4. CONCLUSIONS

The experimental data disclosed that orifice plates placed at 162D, 632D and 886 D downstream the mixer exhibited the same pressure drop for a fixed phases flow rates and area contraction ratio. The lack of influence of an entrance length to the pressure drop in slug flow regime suggests that the pressure drop is defined by the flow structure near the orifice. Consequently, the pressure drop is independent of the slug initiation processes.

The pressure drop across the orifice is quasi-periodic due to the intermittent nature of the slug flow. It is better described by a mean pressure drop plus a fluctuating pressure signal around the mean value. The amplitude of the fluctuating pressure is comparable to the mean value. The characteristic frequencies of the pressure drop is not characterized by a single frequency but for a frequency spectrum which changes as the orifice distance from the mixer or the area contraction ratio changes.

5. REFERENCES

Ahmed, W. H., Ching, C. Y., & Shoukri, M., 2008. "Development of two-phase flow downstream of a horizontal sudden expansion". International Journal of Heat and Fluid Flow, 29(1), 194-206.

Aloui, F., Doubliez, L., Legrand, J., & Souhar, M., 1999. "Bubbly flow in an axisymmetric sudden expansion: Pressure drop, void fraction, wall shear stress, bubble velocities and sizes". Experimental thermal and fluid science, 19(2), 118-130.

Bertola, V., 2004. "The structure of gas-liquid flow in a horizontal pipe with abrupt area contraction". Experimental thermal and fluid science, 28(6), 505-512.

Chen, Y., Chu, M. C., Liaw, J. S., & Wang, C. C., 2008. "Two-phase flow characteristics across sudden contraction in small rectangular channels". Experimental Thermal and Fluid Science, 32(8), 1609-1619.

Chisholm, D., 1983. "Two-phase flow in pipelines and heat exchangers" (p. 110). London: George Godwin.

Dalla Maria, L., 2016. "Estudo Experimental das Ondas de Fração de Vazio e Pressão em Escoamento Horizontal Transiente de Ar e Água no Padrão Intermitente". Master's thesis, Universidade Estadual de Campinas, Campinas, SP, Brazil.

Fossa, M., & Guglielmini, G., 1998. "Dynamic void fraction measurements in horizontal ducts with sudden area contraction". International journal of heat and mass transfer, 41(23), 3807-3815.

Fossa, M., & Guglielmini, G., 2002. "Pressure drop and void fraction profiles during horizontal flow through thin and thick orifices". Experimental Thermal and Fluid Science, 26(5), 513-523.

Fossa, M., Guglielmini, G., & Marchitto, A., 2006. "Two-phase flow structure close to orifice contractions during horizontal intermittent flows". International communications in heat and mass transfer, 33(6), 698-708.

Kojasoy, G., Landis, F., Kwame-Mensah, P., & Chang, C. T., 1997. "Two-phase pressure drop in multiple thick-and thin-orifice plates". Experimental thermal and fluid science, 15(4), 347-358.

Lin, Z. H., 1982. "Two-phase flow measurements with sharp-edged orifices". International Journal of Multiphase Flow, 8(6), 683-693.

Lush, P. A., & Skipp, S. R., 1986. "High speed cine observations of cavitating flow in a duct". International journal of heat and fluid flow, 7(4), 283-290.

Oliveira, J. L. G., Passos, J. C., Verschaeren, R., & van der Geld, C., 2009. “Mass flow rate measurements in gas-liquid flows by means of a venturi or orifice plate coupled to a void fraction sensor”. Experimental Thermal and Fluid Science, 33(2), 253-260.

Petrick, M., & Swanson, B. S., 1959. “Expansion and contraction of an air-water mixture in vertical flow”. AIChE Journal, 5(4), 440-445.

Polonsky, S., Shemer, L., & Barnea, D., 1999. “The relation between the Taylor bubble motion and the velocity field ahead of it”. International Journal of Multiphase Flow, 25(6), 957-975.

Rosa, E. S., & Souza, M. A., 2015. “Spatial void fraction measurement in an upward gas–liquid flow on the slug regime”. Flow Measurement and Instrumentation, 46, 139-154.

Salcudean, M., Groeneveld, D. C., & Leung, L., 1983. “Effect of flow-obstruction geometry on pressure drops in horizontal air-water flow”. International Journal of Multiphase Flow, 9(1), 73-85.

Schmidt, J., & Friedel, L., 1997. “Two-phase pressure drop across sudden contractions in duct areas”. International journal of multiphase flow, 23(2), 283-299.

Taitel, Y., & Barnea, D., 1990. “Two-phase slug flow”. Adv. Heat Transfer, 20, 83-132.

Talvy, C. A., Shemer, L., & Barnea, D., 2000. On the interaction between two consecutive elongated bubbles in a vertical pipe. International Journal of Multiphase Flow, 26(12), 1905-1923.

Thang, N. T., & Davis, M. R., 1981. “Pressure distribution in bubbly flow through venturis”. International Journal of Multiphase Flow, 7(2), 191-210.

Zuber, N., & Findlay, J. A., 1964. “The effects of non-uniform flow and concentration distributions and the effect of the local relative velocity on the average volumetric concentration in two-phase flow”. (No. GEAP-4592; EURAEC-1096). General Electric Co., Schenectady, NY.

6. RESPONSIBILITY NOTICE

The authors are the only responsible for the printed material included in this paper.